BER of OFDM Systems Impaired by Carrier Frequency Offset in Multipath Fading Channels

Luca Rugini, *Member, IEEE*, and Paolo Banelli, *Member, IEEE*

***Abstract*—We introduce an analytical approach to evaluate the error probability of orthogonal frequency-division-multiplexing (OFDM) systems subject to carrier frequency offset (CFO) in frequency-selective channels, characterized by Rayleigh or Rician fading. By properly exploiting the Gaussian approximation of the intercarrier interference (ICI), we show that the bit-error rate (BER) for an uncoded OFDM system with quadrature amplitude modulation (QAM) can be expressed by the sum of a few integrals, whose number depends on the constellation size. Each integral can be evaluated numerically, or, in Rayleigh fading, by using a series expansion that involves generalized hypergeometric functions. Simulation results illustrate that the theoretical analysis is quite accurate, especially for Rayleigh channels, and also with nonlinear amplifiers.**

***Index Terms*—Carrier frequency offset (CFO), fading channels, nonlinear amplifiers, orthogonal frequency-division multiplexing (OFDM).**

I. Introduction

ORTHOGONAL frequency-division multiplexing (OFDM) is a technique widely used for wireless applications [1]. Due to its multicarrier feature, OFDM systems are more sensitive than single-carrier systems to frequency synchronization errors [2]. Indeed, the carrier frequency offset (CFO), which models the frequency mismatch between the transmitter and receiver oscillators, gives rise to intercarrier interference (ICI), thereby destroying the orthogonality of the OFDM data.

In linearly modulated OFDM systems, the performance degradation caused by the CFO, as well as the ICI due to channel Doppler spread, is often evaluated in terms of signal-to-interference-plus-noise ratio (SINR) or signal-to-interference ratio (SIR) [2]–[6]. Although such an analysis has the merit of being mathematically simple, it is obvious that the bit-error rate (BER) or symbol-error rate (SER) analysis characterizes the performance degradation more accurately. In [7], Keller and Hanzo use the Gaussian approximation of the ICI in order to obtain an analytical BER expression in additive white Gaussian noise (AWGN) channels. However, they show by simulation that such an approximation is highly pessimistic when the BER is small, and hence, it should be used only at low signal-to-noise ratio (SNR). A more accurate BER expression that exploits the moments of the ICI distribution has been proposed by Zhao and Häggman in [8]. Moreover, using the characteristic function of the ICI, Sathananthan and Tellambura derived the exact SER in AWGN channels [9].

The main weakness of [7]–[9] is that they consider the CFO effects only in AWGN channels, whereas OFDM systems are usually designed to cope with multipath channels [1]. On this subject, by using the Gaussian approximation of the ICI, Cheon and Hong proposed a BER analysis in Rayleigh fading channels, incorporating both the effects of the CFO and of the channel-estimation errors [10]. The Gaussian approximation of the ICI has been exploited also by Russell and Stüber in [11] to evaluate the BER in the presence of channel Doppler spread.

In this paper, we present a BER analysis when the CFO impairs an OFDM system in frequency-selective Rician or Rayleigh fading channels. Our approach consists of three steps. First, we evaluate the SINR conditioned on a single channel realization. We show that the conditional SINR, which is in general different from the average SINR evaluated in [2]–[4] and [6], strongly depends on the channel realization. Second, we exploit the Gaussian approximation of the ICI to approximate the BER conditioned on the given channel realization. Different from [10], we assume the ICI power as channel dependent. Third, we average the conditional BER over the fading statistics. Our analysis shows that the BER for an uncoded OFDM system with quadrature amplitude modulation (QAM) can be obtained as the sum of a few integrals, whose number depends on the constellation size. Each integral can be computed by numerical techniques, or, in Rayleigh fading, replaced by a series expansion that involves generalized hypergeometric functions. Simulation results in wireless local area network (WLAN) scenarios evidence that, different from the AWGN case [7], for frequency-selective channels, the Gaussian approximation of the ICI is quite appropriate. In particular, for Rayleigh channels, our BER analysis is more accurate than in [10].

The paper is organized as follows. Section II contains the OFDM system model with CFO, while in Section III, we derive the BER expressions for Rayleigh and Rician fading channels. Section IV extends the analysis to take into account the possible presence of nonlinear distortions introduced by the amplifier at the transmitter side. In Section V, we validate the theoretical analysis by means of simulation results, while Section VI concludes the paper.

II. OFDM System Model

Firstly, we introduce some basic notations. We use lower (upper) bold face letters to denote column vectors (matrices),

Manuscript received April 7, 2003; revised January 15, 2004; accepted June 7, 2004. The editor coordinating the review of this paper and approving it for publication is L. Hanzo. This work was supported in part by the Italian Ministry of University and Research, PRIN 2000 Project “Sistemi OFDM con applicazione alle reti WLAN.”

The authors are with the Dipartimento di Ingegneria Elettronica e dell’Informazione, University of Perugia, 06125 Perugia, Italy (e-mail: banelli@diei.unipg.it).

Digital Object Identifier 10.1109/TWC.2005.853884

superscripts *, $^{\mathrm{T}}$, and $^{\mathrm{H}}$ to represent complex conjugate, transpose, and Hermitian operators, respectively. We employ $E\{\cdot\}$ to represent the statistical expectation, $\mathrm{Re}[\cdot]$ to indicate the real part of a complex number, $\max\{a_1,\ldots,a_N\}$ to identify the maximum among the real numbers $a_1,\ldots,a_N$, and $\lceil x \rceil$ and $\lfloor x \rfloor$ to denote the smallest integer greater than or equal to x, and the greatest integer smaller than or equal to x, respectively. The Q-function is defined as $Q(x) = (1/\sqrt{2\pi})\int_x^{+\infty} \mathrm{e}^{-\nu^2/2}\mathrm{d}\nu$, $\mathbf{0}_{M\times N}$ is the $M \times N$ all-zero matrix, $\mathbf{1}_N$ is the N-dimensional all-one column vector, and $\mathbf{I}_N$ is the $N \times N$ identity matrix. We define $[\mathbf{A}]_{m,n}$ as the (m,n)th entry of the matrix $\mathbf{A}$, $[\mathbf{a}]_n$ as the nth entry of the column vector $\mathbf{a}$, $(a)_{\mathrm{mod}\ N}$ as the remainder after division of a by N, and $\mathrm{diag}(\mathbf{a})$ as the diagonal matrix with (n,n)th entry equal to $[\mathbf{a}]_n$.

An OFDM system with N subcarriers and a cyclic prefix of length L is considered. Using a notation similar to [12], the lth transmitted block can be expressed as

$$\mathbf{u}[l] = \mathbf{T}_{\mathrm{CP}}\mathbf{F}^{\mathrm{H}}\mathbf{s}[l] \tag{1}$$

where $\mathbf{u}[l]$ is a vector of dimension $P = N + L$, $\mathbf{F}$ is the $N \times N$ unitary fast Fourier transform (FFT) matrix, defined by $[\mathbf{F}]_{m,n} = N^{-1/2}\exp\{[-j2\pi(m-1)(n-1)]/N\}$, $\mathbf{s}[l]$ is the N-dimensional vector that contains the data symbols, and $\mathbf{T}_{\mathrm{CP}} = [\mathbf{I}_{\mathrm{CP}}^{\mathrm{T}}\mathbf{I}_N^{\mathrm{T}}]^{\mathrm{T}}$ is the $P \times N$ matrix that inserts the cyclic prefix, where $\mathbf{I}_{\mathrm{CP}}$ contains the last L rows of the identity matrix $\mathbf{I}_N$. The data symbols contained in $\mathbf{s}[l]$, drawn from an M-ary square QAM constellation, are assumed to be independent and identically distributed (i.i.d.) with power $\sigma_{\mathrm{S}}^2 = 1$.

After the parallel-to-serial conversion, the signal stream $u[lP+n] = [\mathbf{u}[l]]_n$ is transmitted through a multipath channel, with impulse response expressed by

$$h(t) = \sum_{q=1}^{Q} \zeta_q R_\psi(t - \tau_q) \tag{2}$$

where Q is the number of paths, ζ_q and τ_q are the complex amplitude and the propagation delay, respectively, of the qth path, and $R_\psi(\tau)$ is the autocorrelation function of the pulse-shaping waveform $\psi(t)$. We consider a rectangular pulse-shaping waveform with duration $T_{\mathrm{S}} = T/N$, where T_{S} is the sampling period and $\Delta_f = 1/T$ is the subcarrier spacing. The discrete-time equivalent channel is expressed by

$$h[i] = h(iT_{\mathrm{S}}). \tag{3}$$

Throughout the paper, we assume that the channel amplitudes $\{\zeta_q\}$ of the continuous-time channel (2) are Gaussian distributed. Hence, also the taps of the discrete-time channel (3) are Gaussian distributed, giving rise to Rayleigh or Rician fading depending on their mean value. We also assume that the maximum delay spread $\tau_{\max} = \max\{\tau_q\}$ is smaller than the cyclic-prefix duration $\tau_{\mathrm{CP}} = LT_{\mathrm{S}}$, i.e., $h[i]$ may have nonzero entries only when $0 \le i \le L$.

At the receiver side, the samples obtained after matched filtering can be expressed as [13]

$$x[p] = \mathrm{e}^{j2\pi f_0 pT_{\mathrm{S}}} \sum_{i=0}^{L} h[i]u[p-i] + w[p] \tag{4}$$

where f_0 is the CFO, and $w[p]$ represents the AWGN. Since we want to focus on the effects of the CFO, we will assume that the timing information is available at the receiver. This information could be acquired by exploiting timing-synchronization algorithms designed to work in the presence of an unknown CFO [14]–[16]. In any case, when timing errors are significant, the BER expressions we will derive later can be considered as BER lower bounds.

The P received samples relative to the lth OFDM block are grouped in the vector $\mathbf{x}[l]$, thus obtaining [13]

$$\mathbf{x}[l] = \mathrm{e}^{\frac{j2\pi\varepsilon lP}{N}}\tilde{\mathbf{D}}\left(\mathbf{H}_0\mathbf{u}[l] + \mathbf{H}_1\mathbf{u}[l-1]\right) + \tilde{\mathbf{w}}[l] \tag{5}$$

where $[\mathbf{x}[l]]_n = x[lP+n]$, $\varepsilon = f_0 T$ is the normalized CFO, $\tilde{\mathbf{D}}$ is a $P \times P$ diagonal matrix defined by $[\tilde{\mathbf{D}}]_{n,n} = \mathrm{e}^{j2\pi\varepsilon(n-1)/N}$, and $\mathbf{H}_0$ and $\mathbf{H}_1$ are $P \times P$ Toeplitz matrices defined by [12]

$$\mathbf{H}_0 = \begin{bmatrix} h[0] & 0 & \cdots & \cdots & 0 \\ \vdots & \ddots & \ddots & & \vdots \\ h[L] & & \ddots & \ddots & \vdots \\ \vdots & \ddots & & \ddots & 0 \\ 0 & \cdots & h[L] & \cdots & h[0] \end{bmatrix}$$

$$\mathbf{H}_1 = \begin{bmatrix} 0 & \cdots & h[L] & \cdots & h[1] \\ \vdots & \ddots & & \ddots & \vdots \\ 0 & & \ddots & & h[L] \\ \vdots & \ddots & & \ddots & \vdots \\ 0 & \cdots & 0 & \cdots & 0 \end{bmatrix}. \tag{6}$$

By applying the matrix $\mathbf{R}_{\mathrm{CP}} = [\mathbf{0}_{N\times L}\mathbf{I}_N]$ to $\mathbf{x}[l]$ in (5), the cyclic prefix (and hence, the interblock interference) is eliminated, thus obtaining, by (1), the $N \times 1$ vector [13]

$$\mathbf{y}[l] = \mathbf{R}_{\mathrm{CP}}\mathbf{x}[l] = \mathrm{e}^{\frac{j2\pi\varepsilon(lP+L)}{N}}\mathbf{DHF}^{\mathrm{H}}\mathbf{s}[l] + \mathbf{w}[l] \tag{7}$$

where $\mathbf{D}$ is an $N \times N$ diagonal matrix defined by $[\mathbf{D}]_{n,n} = \mathrm{e}^{j2\pi\varepsilon(n-1)/N}$, $\mathbf{H} = \mathbf{R}_{\mathrm{CP}}\mathbf{H}_0\mathbf{T}_{\mathrm{CP}}$ is the circulant channel matrix defined by $[\mathbf{H}]_{m,n} = h[(m-n)_{\mathrm{mod}\ N}]$, and $\mathbf{w}[l] = \mathbf{R}_{\mathrm{CP}}\tilde{\mathbf{w}}[l]$. By applying the FFT at the receiver, we obtain $\mathbf{z}[l] = \mathbf{F}\mathbf{y}[l]$, which by (7) can be rearranged as

$$\mathbf{z}[l] = \mathrm{e}^{\frac{j2\pi\varepsilon(lP+L)}{N}}\mathbf{\Phi\Lambda s}[l] + \mathbf{v}[l] \tag{8}$$

where $\mathbf{\Phi} = \mathbf{FDF}^{\mathrm{H}}$ is the circulant matrix that produces the ICI, $\mathbf{\Lambda} = \mathbf{FHF}^{\mathrm{H}} = \mathrm{diag}(\boldsymbol{\lambda})$ is the channel diagonal matrix with elements expressed by

$$\boldsymbol{\lambda} = \sqrt{N}\mathbf{Fh} \tag{9}$$

$\mathbf{h} = [h[0]\ \cdots\ h[N-1]]^{\mathrm{T}}$ and $\boldsymbol{\lambda} = [\lambda_1\ \cdots\ \lambda_N]^{\mathrm{T}}$ being the channel vectors in the time domain and frequency domain, respectively, and $\mathbf{v}[l] = \mathbf{F}\mathbf{w}[l] = \mathbf{F}\mathbf{R}_{\mathrm{CP}}\tilde{\mathbf{w}}[l]$ represents the AWGN. From the above definitions, it is straightforward to verify that [9]

$$[\boldsymbol{\Phi}]_{m,n} = \frac{\sin\left(\pi\left((n-m)_{\bmod N} + \varepsilon\right)\right)}{N \sin\left(\frac{\pi}{N}\left((n-m)_{\bmod N} + \varepsilon\right)\right)} \times \mathrm{e}^{j\pi \frac{N-1}{N}\left((n-m)_{\bmod N} + \varepsilon\right)}. \quad (10)$$

Equation (8) shows the combined effect of the CFO and the frequency-selective channel on the received vector $\mathbf{z}[l]$. The only difference, with respect to the AWGN case (i.e., when $\boldsymbol{\Lambda}$ reduces to $\mathbf{I}_N$), is that the CFO matrix $\exp\{[j2\pi\varepsilon(lP + L)]/N\}\boldsymbol{\Phi}$, in frequency-selective channels, acts on the channel-affected data vector $\boldsymbol{\Lambda}\mathbf{s}[l]$ rather than on the original data vector $\mathbf{s}[l]$. Consequently, the presence of a CFO produces similar effects in both AWGN and frequency-selective scenarios, as briefly outlined in the following. First of all, since $\boldsymbol{\Phi}$ is not diagonal, there exists ICI among the channel-affected data. Moreover, since the elements on the main diagonal are characterized by $|[\boldsymbol{\Phi}]_{n,n}| < 1$, the CFO introduces an attenuation of the useful data transmitted on each subcarrier. In addition, the matrix $\boldsymbol{\Phi}$ contains also a phase-shift term $\exp\{[j\pi\varepsilon(N-1)]/N\}$ that is common to all the subcarriers, which has to be added to the block-dependent phase-shift term $\exp\{[j2\pi\varepsilon(lP + L)]/N\}$ in (8).

In this paper, we assume perfect channel state information at the receiver. Moreover, we assume that the receiver is able to perfectly compensate for the aggregate phase-shift term

$$\varphi[l] = \mathrm{e}^{\frac{j2\pi\varepsilon(lP+L)}{N}} \mathrm{e}^{\frac{j\pi\varepsilon(N-1)}{N}} \quad (11)$$

which produces a time-varying rotation of the constellation. Although this hypothesis may appear optimistic, it is a standard assumption [2], because it leads to time-invariant decision regions that correspond to the transmitted constellation. In any case, since the phase shift in (11) is common to all the subcarriers, its estimation can be incorporated into the channel-estimation step. Consequently, if pilot tones are employed, the estimation accuracy depends on the number of dedicated subcarriers.

Thus, by considering the effective channel as expressed by $\varphi[l]\boldsymbol{\Lambda}$, and performing the classical zero-forcing equalization, from (8), we obtain

$$\mathbf{z}_{\mathrm{EQ}}[l] = \varphi[l]^{-1}\boldsymbol{\Lambda}^{-1}\mathbf{z}[l] = \boldsymbol{\Lambda}^{-1}\mathbf{M}\boldsymbol{\Lambda}\mathbf{s}[l] + \mathbf{v}_{\mathrm{EQ}}[l] \quad (12)$$

where $\mathbf{M} = \exp\{[-j\pi\varepsilon(N-1)]/N\}\boldsymbol{\Phi}$ contains the CFO, and $\mathbf{v}_{\mathrm{EQ}}[l] = \varphi[l]^{-1}\boldsymbol{\Lambda}^{-1}\mathbf{v}[l]$. The decision over $\mathbf{z}_{\mathrm{EQ}}[l]$ is successively done according to the proper constellation size M.

III. BER OF OFDM SYSTEMS WITH CFO IN FADING CHANNELS

In order to evaluate the error probability, without loss of generality, we focus on the signal received on the first subcarrier, dropping the block index l for the sake of simplicity. We consider a scaled version of the decision variable, obtained from (12), as expressed by

$$z_1 = \lambda_1 z_{\mathrm{EQ},1} = m_1\lambda_1 s_1 + \sum_{n=2}^{N} m_n\lambda_n s_n + v_1 \quad (13)$$

where $z_{\mathrm{EQ},1} = [\mathbf{z}_{\mathrm{EQ}}[l]]_1$, $s_n = [\mathbf{s}[l]]_n$, $v_1 = \varphi[l]^{-1}[\mathbf{v}[l]]_1$, and

$$m_n = [\mathbf{M}]_{1,n} = \frac{\sin\left(\pi(n-1+\varepsilon)\right)}{N\sin\left(\frac{\pi(n-1+\varepsilon)}{N}\right)}\mathrm{e}^{j\pi\frac{N-1}{N}(n-1)} \quad (14)$$

represents the ICI coefficient due to the nth subcarrier for $n = 2, \ldots, N$, and the attenuation factor of the useful data when $n = 1$.

A possible approach to obtain the BER (or equivalently, the SER) consists of two steps. Firstly, we should calculate the conditional bit-error probability $P_{\mathrm{BE}}(\mathbf{s}, \boldsymbol{\lambda})$ that depends on the symbols in $\mathbf{s} = [s_1 \ \cdots \ s_N]^{\mathrm{T}}$ and on the channel amplitudes in $\boldsymbol{\lambda} = [\lambda_1 \ \cdots \ \lambda_N]^{\mathrm{T}}$. Successively, $P_{\mathrm{BE}}(\mathbf{s}, \boldsymbol{\lambda})$ should be averaged over the joint probability density function (pdf) $f_{\mathrm{S},\Lambda}(\mathbf{s}, \boldsymbol{\lambda}) = f_{\mathrm{S}}(\mathbf{s})f_{\Lambda}(\boldsymbol{\lambda})$ of the symbols and the channel amplitudes, as expressed by

$$\mathrm{BER} = \int_{\mathbf{s},\boldsymbol{\lambda}} P_{\mathrm{BE}}(\mathbf{s}, \boldsymbol{\lambda}) f_{\mathrm{S}}(\mathbf{s}) f_{\Lambda}(\boldsymbol{\lambda}) \mathrm{d}\mathbf{s}\mathrm{d}\boldsymbol{\lambda}. \quad (15)$$

The main difficulty in evaluating (15) is due to the presence of the N-dimensional pdf $f_{\Lambda}(\boldsymbol{\lambda})$. Indeed, when dealing with multidimensional integrations, it would be easier to evaluate many single-variable integrals one at a time. However, (9) shows that the N variables in $\boldsymbol{\lambda}$ are correlated with one another, because the frequency-domain channel is obtained by combining at most $L + 1$ random variables, which are the nonzero entries of $\mathbf{h}$. Therefore, $f_{\Lambda}(\boldsymbol{\lambda})$ cannot be expressed as a product of N separate one-dimensional pdfs. In order to overcome this problem, we bypass the multidimensional integration by using the equality given by $f_{\Lambda}(\boldsymbol{\lambda}) = f_{\overline{\Lambda}|\lambda_1}(\overline{\boldsymbol{\lambda}}|\lambda_1) f_{\boldsymbol{\lambda}_1}(\lambda_1)$, where $f_{\overline{\Lambda}|\lambda_1}(\overline{\boldsymbol{\lambda}}|\lambda_1)$ is the conditional pdf of $\overline{\boldsymbol{\lambda}} = [\lambda_2 \ \cdots \ \lambda_N]^{\mathrm{T}}$ given λ_1, and $f_{\lambda_1}(\lambda_1)$ is the pdf of λ_1. Therefore, (15) becomes

$$\mathrm{BER} = \int_{\lambda_1} P_{\mathrm{BE}}(\lambda_1) f_{\lambda_1}(\lambda_1) \mathrm{d}\lambda_1 \quad (16)$$

where

$$P_{\mathrm{BE}}(\lambda_1) = \int_{\mathbf{s},\overline{\boldsymbol{\lambda}}} P_{\mathrm{BE}}(\mathbf{s}, \boldsymbol{\lambda}) f_{\overline{\Lambda}|\lambda_1}(\overline{\boldsymbol{\lambda}}|\lambda_1) f_{\mathrm{S}}(\mathbf{s}) \mathrm{d}\mathbf{s}\mathrm{d}\overline{\boldsymbol{\lambda}}. \quad (17)$$

In the following, we show that it is possible to approximate $P_{\mathrm{BE}}(\lambda_1)$ without solving the multidimensional integral in (17). Hence, by (16), the BER can be expressed as an integral over a single complex variable.

A. BER Evaluation in Rayleigh Fading Channels

When the channel experiences Rayleigh fading, the channel vector $\mathbf{h}$, and hence $\boldsymbol{\lambda}$ in (9), is a zero-mean complex Gaussian random vector. In this case, the conditional pdf $f_{\overline{\lambda}|\lambda_1}(\overline{\boldsymbol{\lambda}}|\lambda_1)$ is an $(N-1)$-dimensional Gaussian function with mean $\boldsymbol{\eta}_{\overline{\boldsymbol{\lambda}}|\lambda_1}$ and covariance $\mathbf{C}_{\overline{\boldsymbol{\lambda}}|\lambda_1}$ expressed by [17]

$$\boldsymbol{\eta}_{\overline{\boldsymbol{\lambda}}|\lambda_1} = \lambda_1 c^{-1}_{\lambda_1\lambda_1}\mathbf{c}_{\overline{\boldsymbol{\lambda}}\lambda_1} \tag{18}$$

$$\mathbf{C}_{\overline{\boldsymbol{\lambda}}|\lambda_1} = \mathbf{C}_{\overline{\boldsymbol{\lambda}}\,\overline{\boldsymbol{\lambda}}} - c^{-1}_{\lambda_1\lambda_1}\mathbf{c}_{\overline{\boldsymbol{\lambda}}\lambda_1}\mathbf{c}^{\mathrm{H}}_{\overline{\boldsymbol{\lambda}}\lambda_1} \tag{19}$$

where $c_{\lambda_i\lambda_j} = E\{\lambda_i\lambda_j^*\}$, $\mathbf{c}_{\overline{\boldsymbol{\lambda}}\lambda_1} = [c_{\lambda_2\lambda_1} \ \cdots \ c_{\lambda_N\lambda_1}]^{\mathrm{T}}$, and $\mathbf{C}_{\overline{\boldsymbol{\lambda}}\,\overline{\boldsymbol{\lambda}}}$ is the $(N-1)$-dimensional square matrix extracted from

$$\mathbf{C}_{\boldsymbol{\lambda}\boldsymbol{\lambda}} = E\{\boldsymbol{\lambda}\boldsymbol{\lambda}^{\mathrm{H}}\} = \begin{bmatrix} c_{\lambda_1\lambda_1} & \mathbf{c}^{\mathrm{H}}_{\overline{\boldsymbol{\lambda}}\lambda_1} \\ \mathbf{c}_{\overline{\boldsymbol{\lambda}}\lambda_1} & \mathbf{C}_{\overline{\boldsymbol{\lambda}}\,\overline{\boldsymbol{\lambda}}} \end{bmatrix} \tag{20}$$

which is the covariance matrix of the frequency-domain channel, related to the covariance matrix $\mathbf{C}_{\mathbf{hh}} = E\{\mathbf{hh}^{\mathrm{H}}\}$ of the time-domain channel by $\mathbf{C}_{\boldsymbol{\lambda}\boldsymbol{\lambda}} = N\mathbf{F}\mathbf{C}_{\mathbf{hh}}\mathbf{F}^{\mathrm{H}}$. After defining the conditional random variable $t_1 = z_1|\lambda_1$, from (13), we obtain

$$t_1 = m_1\lambda_1 s_1 + \sum_{n=2}^{N} m_n k_n s_n + v_1 \tag{21}$$

where the conditional random variable $k_n = \lambda_n|\lambda_1$ is Gaussian, with mean value $\eta_n = E\{k_n\}$ obtained from (18) as $\eta_n = \lambda_1 c^{-1}_{\lambda_1\lambda_1} c_{\lambda_n\lambda_1}$, and with variance obtained from (19) as $\sigma_n^2 = [\mathbf{C}_{\overline{\boldsymbol{\lambda}}|\lambda_1}]_{n-1,n-1}$, $n = 2,\ldots,N$. Consequently, by defining the zero-mean random variable $\kappa_n = k_n - \eta_n$, we obtain

$$t_1 = m_1\lambda_1 s_1 + \alpha_1\lambda_1 + \beta_1 + v_1 \tag{22}$$

where, by means of (18)

$$\alpha_1 = c^{-1}_{\lambda_1\lambda_1}\sum_{n=2}^{N} m_n c_{\lambda_n\lambda_1} s_n \tag{23}$$

$$\beta_1 = \sum_{n=2}^{N} m_n \kappa_n s_n. \tag{24}$$

The quantities α_1 and β_1 depend on the statistical characterization of the channel in the frequency domain, which is contained in $c^{-1}_{\lambda_1\lambda_1} c_{\lambda_n\lambda_1}$ and in κ_n, respectively, on the normalized CFO ε, which is linked to m_n by (14), and on the transmitted symbols $\{s_n\}$ corresponding to the interfering subcarriers $n = 2,\ldots,N$. It can be observed that α_1 in (23) depends on the correlation terms $c_{\lambda_n\lambda_1}$ among the subcarriers deterministically, while β_1 in (24) depends on the correlation terms $c_{\lambda_n\lambda_1}$ statistically, by the variance of κ_n that is equal to $\sigma_n^2 = [\mathbf{C}_{\overline{\boldsymbol{\lambda}}|\lambda_1}]_{n-1,n-1}$. Anyway, α_1 and β_1 do not depend on the specific value of λ_1 that characterizes the channel realization.

From (22)–(24), it is evident that the ICI consists of two parts. The first one ($\alpha_1\lambda_1$) is proportional to the channel amplitude λ_1 of the useful signal. Hence, $\alpha_1\lambda_1$ represents the ICI part that fades synchronously with the useful signal. The power of $\alpha_1\lambda_1$, which obviously depends on λ_1, can be expressed as $|\lambda_1|^2\sigma^2_{\mathrm{ICI},\alpha}$, where

$$\sigma^2_{\mathrm{ICI},\alpha} = \left|c^{-1}_{\lambda_1\lambda_1}\right|^2 \sum_{n=2}^{N} \left|m_n c_{\lambda_n\lambda_1}\right|^2. \tag{25}$$

On the other hand, the second part (β_1) has a power that is independent of λ_1, and only depends on $\mathbf{C}_{\overline{\boldsymbol{\lambda}}|\lambda_1}$, as expressed by

$$\sigma^2_{\mathrm{ICI},\beta} = \sum_{n=2}^{N} |m_n|^2\sigma_n^2 = \sum_{n=2}^{N} |m_n|^2[\mathbf{C}_{\overline{\boldsymbol{\lambda}}|\lambda_1}]_{n-1,n-1}. \tag{26}$$

Since $\alpha_1\lambda_1$ and β_1 are uncorrelated, the SINR conditioned on λ_1 can be expressed as

$$\gamma(\lambda_1) = \frac{|\lambda_1|^2|m_1|^2}{|\lambda_1|^2\sigma^2_{\mathrm{ICI},\alpha} + \sigma^2_{\mathrm{ICI},\beta} + \sigma^2_{\mathrm{AWGN}}} \tag{27}$$

where $\sigma^2_{\mathrm{ICI},\alpha}$ and $\sigma^2_{\mathrm{ICI},\beta}$ are expressed by (25) and (26), respectively, and $\sigma^2_{\mathrm{AWGN}} = E\{|v_1|^2\}$. We underline that the SINR expression (27) is conditioned on the specific channel gain λ_1, and therefore, it does not coincide with the average SINR evaluated in other papers (e.g., [2]–[4] and [6]). Moreover, the conditional SINR expression (27) is valid also when the paths of the channel in (2) are correlated in the time domain. Indeed, both (25) and (26) take into account the frequency-domain channel correlation, which is also influenced by a possible channel correlation in the time domain. In addition, since we consider time-invariant channels, our expression does not include Doppler-spread effects, which are considered in [5] and [6].

It is worth noting that, when the channel experiences frequency-flat fading, all the ICI is contained in $\alpha_1\lambda_1$, because in this case all the subcarriers fade simultaneously. Indeed, when $\lambda_n = \lambda_1 \forall n \in \{1,\ldots,N\}$, by comparing (13) with (22), it holds true that $\alpha_1 = \sum_{n=2}^{N} m_n s_n$ and $\beta_1 = 0$. On the other extreme, $\alpha_1 = 0$ implies that $\mathbf{c}_{\overline{\boldsymbol{\lambda}}\lambda_1} = \mathbf{0}_{N-1\times 1}$, i.e., that the first subcarrier fades independently of the other subcarriers. However, the condition of independent fading is not realistic for all the subcarriers, because a diagonal $\mathbf{C}_{\boldsymbol{\lambda}\boldsymbol{\lambda}}$ implies a circulant $\mathbf{C}_{\mathbf{hh}}$, which is not compatible with the usual hypothesis that the cyclic-prefix length is shorter than the OFDM data block, i.e., $L < N$.

Although α_1 in (23) is not strictly Gaussian, we observe that α_1 is obtained by the linear combination of the i.i.d. data symbols $\{s_n\}_{n=2}^{N}$ with the coefficients $\{m_n c_{\lambda_n\lambda_1}\}_{n=2}^{N}$, apart from the scalar quantity $c^{-1}_{\lambda_1\lambda_1}$. As a consequence, since practical OFDM systems have a high number N of subcarriers [1], the central limit theorem [18] allows the approximation of α_1 as a Gaussian random variable with zero mean and variance $\sigma^2_{\mathrm{ICI},\alpha}$ expressed by (25).

As far as the second part of the ICI is concerned, β_1 in (24) is a linear combination of the random variables $\{\kappa_n s_n\}_{n=2}^{N}$. It can be easily proven [18] that the pdf of $\kappa_n s_n$ is a weighted sum of Gaussian functions, each with variance equal to $E\{|\kappa_n|^2\}|s_n|^2$. Thus, due to the channel correlation in the frequency domain, the pdf of β_1 is not Gaussian. Anyway, we can invoke the central limit theorem to approximate also β_1 as Gaussian, with zero mean and variance expressed by (26).

As pointed out in Section I, the Gaussian approximation of the ICI produced by the CFO has been already exploited in [7] for AWGN channels and in [10] for Rayleigh fading channels. However, in our case, different from [10], the power of the ICI depends on the specific channel realization. In Section V, we will check the accuracy of the approximation employed in our approach.

By exploiting the Gaussian approximation, for QAM modulations with Gray coding, the conditional BER $P_{\mathrm{BE}}(\lambda_1)$ in (17) can be approximated by the standard BER expression for additive Gaussian noise. For example, the conditional BER for QPSK, i.e., 4-QAM, is expressed by

$$P_{\mathrm{BE}}(\lambda_1) = Q\left(\sqrt{\gamma(\lambda_1)}\right) \tag{28}$$

while for 16-QAM it can be expressed by [19]

$$P_{\mathrm{BE}}(\lambda_1) = \frac{3}{4}Q\left(\sqrt{\frac{1}{5}\gamma(\lambda_1)}\right) + \frac{1}{2}Q\left(\sqrt{\frac{9}{5}\gamma(\lambda_1)}\right) - \frac{1}{4}Q\left(\sqrt{5\gamma(\lambda_1)}\right) \tag{29}$$

where $\gamma(\lambda_1)$ is the conditional SINR expressed by (27). In the general M-QAM case, the conditional BER is the sum of $\sqrt{M}-1$ Q-shaped functions, as expressed by

$$P_{\mathrm{BE}}(\lambda_1) = \sum_{i=1}^{\sqrt{M}-1} a_i Q\left(\sqrt{b_i\gamma(\lambda_1)}\right) \tag{30}$$

where the coefficients $\{a_i\}$ and $\{b_i\}$ depend on the constellation size M [19]. Hence, the BER, obtained by inserting (27) and (30) in (16), is the sum of $\sqrt{M}-1$ integrals, as expressed by

$$\mathrm{BER} = \sum_{i=1}^{\sqrt{M}-1} a_i \int_{\lambda_1} Q\left(\sqrt{b_i\gamma(\lambda_1)}\right) f_{\lambda_1}(\lambda_1)\mathrm{d}\lambda_1 \tag{31}$$

where $f_{\lambda_1}(\lambda_1)$ is the complex Gaussian pdf of λ_1.

Without loss of generality, let us now focus on the QPSK case. By (27), it is evident that the conditional SINR, and hence, the conditional probability $P_{\mathrm{BE}}(\lambda_1)$ in (28), depends on $|\lambda_1|$, which is a real random variable with Rayleigh statistic. Therefore, by a suitable change of integration variable, the BER becomes

$$\mathrm{BER} = \int_0^{+\infty} Q\left(\sqrt{\frac{|\lambda_1|^2|m_1|^2}{|\lambda_1|^2\sigma^2_{\mathrm{ICI},\alpha} + \sigma^2_{\mathrm{ICI},\beta} + \sigma^2_{\mathrm{AWGN}}}}\right) \times \frac{2|\lambda_1|}{c_{\lambda_1\lambda_1}} \exp\left(-\frac{|\lambda_1|^2}{c_{\lambda_1\lambda_1}}\right) \mathrm{d}|\lambda_1| \tag{32}$$

which can be solved by numerical techniques such as the Laguerre–Gauss quadrature [20], or estimated by Monte Carlo methods. Alternatively, the integral (32) can be expressed as the series expansion [21]

$$\mathrm{BER} = \frac{1}{2} - \frac{\sqrt{2}\mu}{4}\mathrm{e}^{-\frac{\mu^2}{2\nu^2}} \sum_{k=0}^{+\infty} \frac{1}{k!}\left(\frac{\mu^2}{2\nu^2}\right)^k \times {}_2F_0\left(k+\frac{3}{2}, \frac{1}{2};;-\nu^2\right) \tag{33}$$

where

$$\mu^2 = \frac{c_{\lambda_1\lambda_1}|m_1|^2}{\sigma^2_{\mathrm{ICI},\beta} + \sigma^2_{\mathrm{AWGN}}} \tag{34}$$

$$\nu^2 = \frac{c_{\lambda_1\lambda_1}\sigma^2_{\mathrm{ICI},\alpha}}{\sigma^2_{\mathrm{ICI},\beta} + \sigma^2_{\mathrm{AWGN}}} \tag{35}$$

and ${}_2F_0(a,b;;x) = \sum_{q=0}^{+\infty}(a)_q(b)_q(x^q/q!)$ represents the generalized hypergeometric function [22], where $(a)_q = \Gamma(a+q)/\Gamma(a)$ is the Pochhammer's symbol expressed by means of the Gamma function $\Gamma(\cdot)$ [20]. The proof of the equivalence between (32) and (33) can be found in [21], which also contains a simple and accurate truncation criterion for the series expansion. Indeed, the relevant terms in (33) are only the ones between $k_{\min}$ and $k_{\max}$, expressed by

$$k_{\min} = \max\left\{0, \left\lfloor r - \frac{3}{2\sqrt{2\pi}t}\right\rfloor\right\} \tag{36}$$

$$k_{\max} = \left\lceil r + \frac{3}{2\sqrt{2\pi}t}\right\rceil \tag{37}$$

$$r = \frac{\mu^2}{2\nu^2} \tag{38}$$

$$t = \frac{\sqrt{2}\mu}{4}\mathrm{e}^{-r}\frac{1}{\lfloor r\rfloor!}r^{\lfloor r\rfloor} \times {}_2F_0\left(\lfloor r\rfloor + \frac{3}{2}, \frac{1}{2};;-\nu^2\right). \tag{39}$$

B. BER Evaluation in Rician Fading Channels

In Rician channels, we assume, as usual, that a single line-of-sight (LOS) is present in the time domain, and consequently, the LOS term is the same for all the subcarriers. To evaluate the BER, we use the same approach adopted in the Rayleigh case. Thus, the conditional pdf $f_{\overline{\Lambda}|\lambda_1}(\overline{\boldsymbol{\lambda}}|\lambda_1)$ is still an $(N-1)$-dimensional Gaussian with the same covariance matrix $\mathbf{C}_{\overline{\boldsymbol{\lambda}}|\lambda_1}$ expressed by (19), but with a mean value expressed by [17]

$$\boldsymbol{\eta}_{\overline{\boldsymbol{\lambda}}|\lambda_1} = \lambda_{\mathrm{LOS}}\mathbf{1}_{N-1} + \lambda_{1,\mathrm{NLOS}}c^{-1}_{\lambda_1\lambda_1}\mathbf{c}_{\overline{\boldsymbol{\lambda}}\lambda_1} \tag{40}$$

where $\lambda_{\mathrm{LOS}} = E\{\lambda_1\}$, and $\lambda_{1,\mathrm{NLOS}} = \lambda_1 - \lambda_{\mathrm{LOS}}$ is just the zero-mean normalization of the complex Gaussian random variable λ_1. By using t_1 to represent the random variable z_1 conditioned on $\lambda_1 = \lambda_{\mathrm{LOS}} + \lambda_{1,\mathrm{NLOS}}$, we obtain

$$t_1 = m_1\lambda_1 s_1 + \sum_{n=2}^{N} m_n k_n s_n + v_1 \tag{41}$$

where the conditional random variable $k_n = \lambda_n|\lambda_1$ is Gaussian with mean value $\eta_n = \lambda_{\text{LOS}} + \lambda_{1,\text{NLOS}} c^{-1}_{\lambda_1\lambda_1} c_{\lambda_n\lambda_1}$. In this case, t_1 can be expressed as

$$t_1 = m_1\lambda_{\text{LOS}} s_1 + m_1\lambda_{1,\text{NLOS}} s_1 + \alpha_1\lambda_{1,\text{NLOS}} + \chi_1 + \beta_1 + v_1 \quad (42)$$

where

$$\chi_1 = \lambda_{\text{LOS}} \sum_{n=2}^{N} m_n s_n \quad (43)$$

and α_1 and β_1 are defined in (23) and (24), respectively. Equation (42) tells us that the conditional variable t_1 is the sum of a useful term and four noise terms, which, different from the Rayleigh case, are not all uncorrelated with one another. Specifically, the term $\alpha_1\lambda_{1,\text{NLOS}}$ is correlated with χ_1, as expressed by

$$\begin{aligned}\rho_{\text{ICI},\alpha,\chi}&(\lambda_{\text{LOS}}, \lambda_{1,\text{NLOS}}) \\ &= E\{\chi_1^* \alpha_1 \lambda_{1,\text{NLOS}}\} \\ &= c^{-1}_{\lambda_1\lambda_1} \lambda_{1,\text{NLOS}} \lambda^*_{\text{LOS}} \sum_{n=2}^{N} |m_n|^2 c_{\lambda_n\lambda_1}. \end{aligned} \quad (44)$$

By exploiting the Gaussian approximation for α_1, β_1, and χ_1, and taking into account that $\lambda_1 = \lambda_{\text{LOS}} + \lambda_{1,\text{NLOS}}$, the conditional BER $P_{\text{BE}}(\lambda_1)$ is again expressed as the sum of Q-type functions like the one in (30), with conditional SINR given by (45), shown at the bottom of the page, where

$$\sigma^2_{\text{ICI},\chi} = |\lambda_{\text{LOS}}|^2 \sum_{n=2}^{N} |m_n|^2. \quad (46)$$

Therefore, also in the Rician case, the BER can be obtained by numerical integration of (16). For QPSK, this integral is expressed by

$$\text{BER} = \int_{\lambda_{1,\text{NLOS}}} Q\left(\sqrt{\gamma(\lambda_{\text{LOS}}, \lambda_{1,\text{NLOS}})}\right) \times f_{\lambda_{1,\text{NLOS}}}(\lambda_{1,\text{NLOS}}) \mathrm{d}\lambda_{1,\text{NLOS}} \quad (47)$$

where $f_{\lambda_{1,\text{NLOS}}}(\lambda_{1,\text{NLOS}})$ is complex Gaussian with zero mean. Obviously, the BER also depends on the Rician factor K that determines the LOS term λ_{LOS}.

C. BER Evaluation in the Presence of Guard Bands

So far, we have assumed that all the N subcarriers are active, although any practical OFDM system contains some virtual (or null) subcarriers used as guard frequency bands [1]. However, it is easy to extend the BER analysis in order to take into account the presence of V virtual subcarriers, because a virtual subcarrier does not contribute to the ICI. As an example, assume that the null subcarriers are those with $n \in \{N - V + 1, N - V + 2, \ldots, N\}$. The only modification to the previous analysis is that $s_n = 0$ for these subcarriers. Therefore, the BER analysis still remains valid, provided that (25), (26), (44), and (46) are truncated up to $n = N - V$. Obviously, in this case, the BER is not the same for all the active subcarriers, because the ICI power is smaller for those subcarriers that are closer to the guard bands.

IV. BER of OFDM Systems With Both CFO and Nonlinear Distortions in Fading Channels

In this section, we extend the system model and the performance analysis in order to also take into account the nonlinear effects that may be introduced by the high-power amplifier (HPA) at the transmitter side. After passing through an instantaneous HPA, by exploiting the Bussgang theorem, the lth transmitted OFDM block can be modeled by [23], [24]

$$\mathbf{u}[l] = A_0 \mathbf{T}_{\text{CP}} \mathbf{F}^{\text{H}} \mathbf{s}[l] + \mathbf{T}_{\text{CP}} \mathbf{w}_{\text{NL}}[l] \quad (48)$$

where A_0 represents the average linear amplification gain, and $\mathbf{T}_{\text{CP}}\mathbf{w}_{\text{NL}}[l]$ is the nonlinear-distortion noise, uncorrelated with the linear part $A_0\mathbf{T}_{\text{CP}}\mathbf{F}^{\text{H}}\mathbf{s}[l]$. The validity of (48), based on a Gaussian distribution of $\mathbf{F}^{\text{H}}\mathbf{s}[l]$, is justified by the high number of subcarriers usually employed in OFDM systems (e.g., $N > 32$) [24].

By revising the system model with (48) instead of (1), (8) and (13) become

$$\mathbf{z}[l] = A_0 \mathrm{e}^{\frac{j2\pi\varepsilon(lP+L)}{N}} \boldsymbol{\Phi\Lambda}\mathbf{s}[l] + \mathrm{e}^{\frac{j2\pi\varepsilon(lP+L)}{N}} \boldsymbol{\Phi\Lambda}\mathbf{v}_{\text{NL}}[l] + \mathbf{v}[l] \quad (49)$$

$$z_1 = A_0 m_1 \lambda_1 s_1 + A_0 \sum_{n=2}^{N} m_n\lambda_n s_n + \sum_{n=1}^{N} m_n \lambda_n v_{\text{NL},n} + v_1 \quad (50)$$

respectively, where $v_{\text{NL},n} = [\mathbf{v}_{\text{NL}}[l]]_n$, with $\mathbf{v}_{\text{NL}}[l] = \mathbf{F}\mathbf{w}_{\text{NL}}[l]$. Therefore, the BER can still be expressed by (16), with a conditional BER $P_{\text{BE}}(\lambda_1)$ modified to

$$P_{\text{BE}}(\lambda_1) = \int_{\mathbf{s},\mathbf{v}_{\text{NL}},\overline{\boldsymbol{\lambda}}} P_{\text{BE}}(\mathbf{s}, \mathbf{v}_{\text{NL}}, \boldsymbol{\lambda}) f_{\overline{\Lambda}|\lambda_1}(\overline{\boldsymbol{\lambda}}|\lambda_1) \times f_{\text{S},\text{V}_{\text{NL}}}(\mathbf{s}, \mathbf{v}_{\text{NL}}) \mathrm{d}\mathbf{s}\mathrm{d}\mathbf{v}_{\text{NL}}\mathrm{d}\overline{\boldsymbol{\lambda}}. \quad (51)$$

$$\gamma(\lambda_{\text{LOS}}, \lambda_{1,\text{NLOS}}) = \frac{|\lambda_{\text{LOS}} + \lambda_{1,\text{NLOS}}|^2 |m_1|^2}{|\lambda_{1,\text{NLOS}}|^2 \sigma^2_{\text{ICI},\alpha} + 2\text{Re}\left[\rho_{\text{ICI},\alpha,\chi}(\lambda_{\text{LOS}}, \lambda_{1,\text{NLOS}})\right] + \sigma^2_{\text{ICI},\chi} + \sigma^2_{\text{ICI},\beta} + \sigma^2_{\text{AWGN}}} \quad (45)$$

By assuming Rayleigh fading, from (50), the conditional random variable $t_1 = z_1|\lambda_1$ becomes

$$t_1 = A_0(m_1\lambda_1 s_1 + \alpha_1\lambda_1 + \beta_1) + \tilde{\alpha}_1\lambda_1 + \tilde{\beta}_1 + v_1 \quad (52)$$

where α_1 and β_1 are expressed by (23) and (24), respectively, and

$$\tilde{\alpha}_1 = c_{\lambda_1\lambda_1}^{-1}\sum_{n=1}^{N} m_n c_{\lambda_n\lambda_1} v_{\mathrm{NL},n} \quad (53)$$

$$\tilde{\beta}_1 = \sum_{n=2}^{N} m_n \kappa_n v_{\mathrm{NL},n}. \quad (54)$$

Since each element of the nonlinear-distortion noise vector $\mathbf{v}_{\mathrm{NL}}[l] = \mathbf{F}\mathbf{w}_{\mathrm{NL}}[l]$ is obtained by linear combination of N elements, when N is large, the pdf of $\mathbf{v}_{\mathrm{NL}}[l]$ can be approximated by an N-dimensional Gaussian with zero mean and covariance expressed by $\mathbf{C}_{\mathrm{NL}} = E\{\mathbf{v}_{\mathrm{NL}}[l]\mathbf{v}_{\mathrm{NL}}[l]^{\mathrm{H}}\}$. Therefore, by exploiting the uncorrelatedness between the nonlinear-distortion noise and the useful term, it is straightforward to obtain the BER as in (30), with conditional SINR expressed by (55), shown at the bottom of the page, where

$$\sigma_{\mathrm{NL},\alpha}^2 = \left|c_{\lambda_1\lambda_1}^{-1}\right|^2 \sum_{i=1}^{N}\sum_{j=1}^{N} m_i m_j^* c_{\lambda_i\lambda_1} c_{\lambda_j\lambda_1}^* [\mathbf{C}_{\mathrm{NL}}]_{i,j} \quad (56)$$

$$\sigma_{\mathrm{NL},\beta}^2 = \sum_{i=2}^{N}\sum_{j=2}^{N} m_i m_j^* \left[\mathbf{C}_{\overline{\boldsymbol{\lambda}}|\lambda_1}\right]_{i-1,j-1} [\mathbf{C}_{\mathrm{NL}}]_{i,j}. \quad (57)$$

The elements of $\mathbf{C}_{\mathrm{NL}}$, as well as the linear gain A_0, can be evaluated by means of closed-form expressions that depend on the autocorrelation function of the HPA input, on the input backoff (IBO) B_{IN} to the HPA, and on the amplitude modulation to amplitude modulation (AM/AM) and the amplitude modulation to phase modulation (AM/PM) curves of the HPA [23]. Moreover, since the nonlinear-distortion noise has an almost-flat power spectral density in the bandwidth of the useful signal, we can use the approximation $\mathbf{C}_{\mathrm{NL}} \approx \sigma_{\mathrm{NL}}^2 \mathbf{I}_N$, with σ_{NL}^2 calculated as $\sigma_{\mathrm{NL}}^2 = (1/N)\sum_{n=1}^{N}[\mathbf{C}_{\mathrm{NL}}]_{n,n}$ [23]. Therefore, (56) and (57) become

$$\sigma_{\mathrm{NL},\alpha}^2 \approx \sigma_{\mathrm{NL}}^2\left(|m_1|^2 + \sigma_{\mathrm{ICI},\alpha}^2\right) \quad (58)$$

$$\sigma_{\mathrm{NL},\beta}^2 \approx \sigma_{\mathrm{NL}}^2 \sigma_{\mathrm{ICI},\beta}^2 \quad (59)$$

and the conditional SINR (55) can be approximated as

$$\gamma(\lambda_1) \approx \frac{|\lambda_1|^2|A_0|^2|m_1|^2}{|\lambda_1|^2\sigma_\alpha^2 + \sigma_\beta^2 + \sigma_{\mathrm{AWGN}}^2} \quad (60)$$

where

$$\sigma_\alpha^2 = \left(|A_0|^2 + \sigma_{\mathrm{NL}}^2\right)\sigma_{\mathrm{ICI},\alpha}^2 + \sigma_{\mathrm{NL}}^2|m_1|^2 \quad (61)$$

$$\sigma_\beta^2 = \left(|A_0|^2 + \sigma_{\mathrm{NL}}^2\right)\sigma_{\mathrm{ICI},\beta}^2. \quad (62)$$

Also, in this case, we can avoid the numerical integration by resorting to series expansions of ${}_2F_0$-type generalized hypergeometric functions like the one in (33). In this case, by assuming QPSK with Gray coding, the BER is expressed by

$$\mathrm{BER} \approx \frac{1}{2} - \frac{\sqrt{2}\mu}{4}\mathrm{e}^{-\frac{\mu^2}{2\nu^2}}\sum_{k=0}^{+\infty}\frac{1}{k!}\left(\frac{\mu^2}{2\nu^2}\right)^k \times {}_2F_0\left(k+\frac{3}{2}, \frac{1}{2};;-\nu^2\right) \quad (63)$$

where

$$\mu^2 = \frac{c_{\lambda_1\lambda_1}|A_0|^2|m_1|^2}{\sigma_\beta^2 + \sigma_{\mathrm{AWGN}}^2} \quad (64)$$

$$\nu^2 = \frac{c_{\lambda_1\lambda_1}\sigma_\alpha^2}{\sigma_\beta^2 + \sigma_{\mathrm{AWGN}}^2} \quad (65)$$

with σ_α^2 and σ_β^2 expressed by (61) and (62), respectively.

The performance analysis in the presence of nonlinear distortions for Rician channels can be obtained as follows. Firstly, from (50), we can evaluate the conditional random variable $t_1 = z_1|\lambda_1$ by using the same approach adopted for Rician channels in linear scenarios. Successively, like for Rayleigh channels, we can exploit the Gaussian approximation of the nonlinear-distortion noise in order to get the conditional SINR. Both the approaches are very similar to the ones already described in Section III-B and in this section, and therefore, for the sake of brevity, a detailed derivation is omitted.

V. Simulation Results

In this section, we present some simulation results in order to validate the Gaussian approximation of the ICI applied in the theoretical analysis. We consider an OFDM system with $N = 64$ subcarriers, with a subcarrier separation of $\Delta_f = 1/T = 312.5$ kHz, and with cyclic prefix of length $L = 16$. We use the channel models B and D of the IEEE 802.11a WLAN standard [25]. In the models B and D, each time-domain tap suffers independent Rayleigh and Rician fading, respectively, with exponentially decaying power delay profile, and root mean square (rms) delay spread equal to 100 and 140 ns, respectively.

Fig. 1 shows the BER performance of QPSK in the Rayleigh channel B, as a function of the received $(E_{\mathrm{b}}/N_0) = (c_{\lambda_1\lambda_1}/\sigma_{\mathrm{AWGN}}^2 \log_2 M)$. It is evident that the theoretical analysis exactly predicts the simulated BER for different

$$\gamma(\lambda_1) = \frac{|\lambda_1|^2|A_0|^2|m_1|^2}{|\lambda_1|^2|A_0|^2\sigma_{\mathrm{ICI},\alpha}^2 + |A_0|^2\sigma_{\mathrm{ICI},\beta}^2 + |\lambda_1|^2\sigma_{\mathrm{NL},\alpha}^2 + \sigma_{\mathrm{NL},\beta}^2 + \sigma_{\mathrm{AWGN}}^2} \quad (55)$$

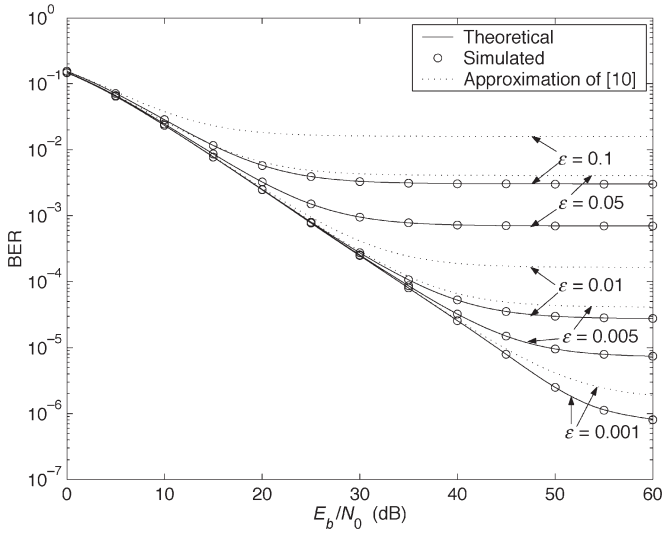

Fig. 1. BER of QPSK in the Rayleigh channel B.

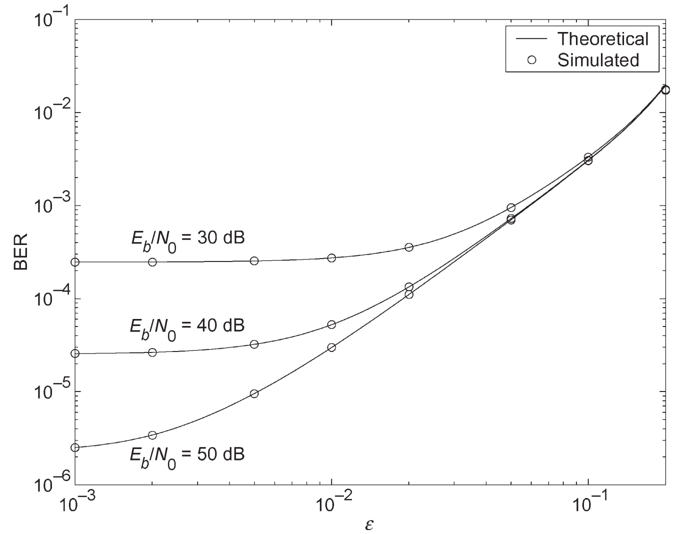

Fig. 3. BER of QPSK in the Rayleigh channel B.

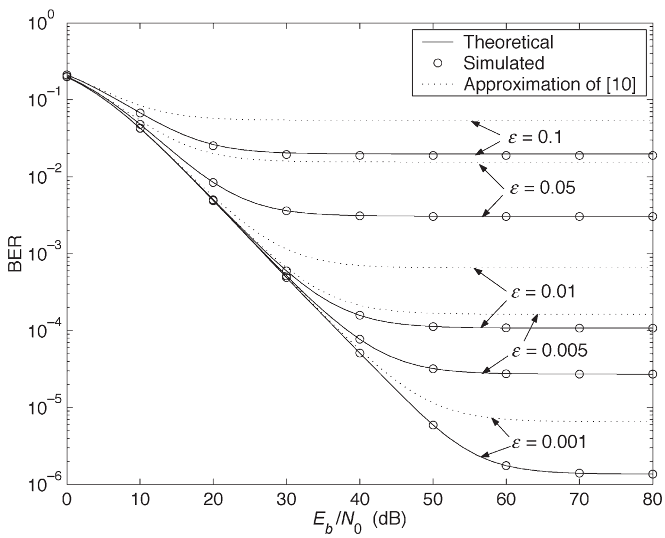

Fig. 2. BER of 16-QAM in the Rayleigh channel B.

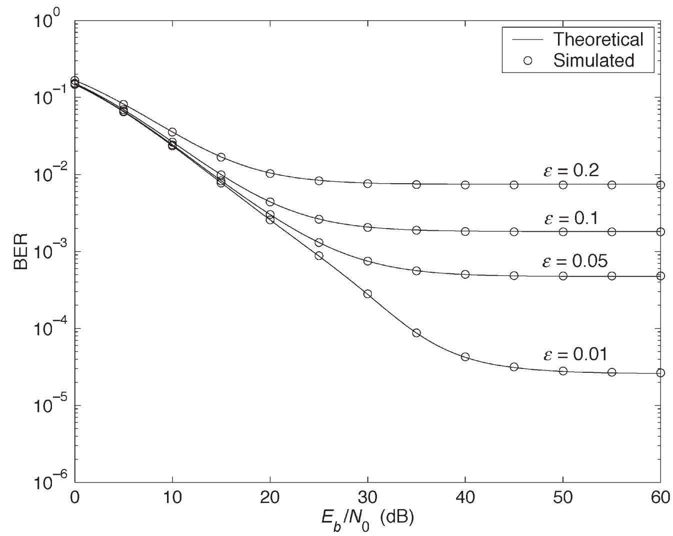

Fig. 4. BER of QPSK in the presence of guard bands.

values of the normalized CFO ε. Such a good agreement clearly indicates that, different from the AWGN case [7], in frequency-selective scenarios, the Gaussian approximation of the ICI leads to accurate results. The motivation of this accuracy can be easily explained. Indeed, when the interference is the sum of many variables, the approximation by a single Gaussian random variable gets worse at the tail of the Gaussian pdf, and consequently, the approximated BER is not sufficiently accurate when the true BER is small (i.e., when the interference power is small compared to the signal power). The mismatch between the approximated and the exact BER happens not only in AWGN channels, but also for the conditional BER $P_{\mathrm{BE}}(\lambda_1)$ in our scenario. However, in fading channels, the BER is obtained by averaging $P_{\mathrm{BE}}(\lambda_1)$ over the pdf of λ_1, and hence, it is practically imposed by the values of $P_{\mathrm{BE}}(\lambda_1)$ that correspond to the small values of $|\lambda_1|$ [26]. For these values, the Gaussian approximation is very good, because $P_{\mathrm{BE}}(\lambda_1)$ is high (i.e., the interference power is significant with respect to the signal power), and therefore, the obtained BER exactly matches with the true BER. This behavior is confirmed by the results of Fig. 2, which shows the BER of 16-QAM versus E_{b}/N_0 for different values of the normalized CFO ε, and by the results of Fig. 3, which exhibits the BER of QPSK versus the normalized CFO ε for different values of E_{b}/N_0.

Figs. 1 and 2 show also the BER performance obtained using the ICI approximation proposed in [10]. Although the paper [10] mainly deals with the effect of the channel-estimation errors, it approximates all the ICI as a zero-mean Gaussian random variable with power independent of the fading gain. However, as we showed in (22), part of the ICI is proportional to the fading gain λ_1. Therefore, when $|\lambda_1|$ is low (high), the ICI power is smaller (larger) than the one assumed in [10]. Since most of the errors are committed when $|\lambda_1|$ is low, it turns out that in [10], the degradation due to the ICI is overestimated, as confirmed by the BER floors in Figs. 1 and 2.

Fig. 4 shows the BER when $N_{\mathrm{A}} = N - V = 52$ out of $N = 64$ subcarriers are active [25], using QPSK and channel B.

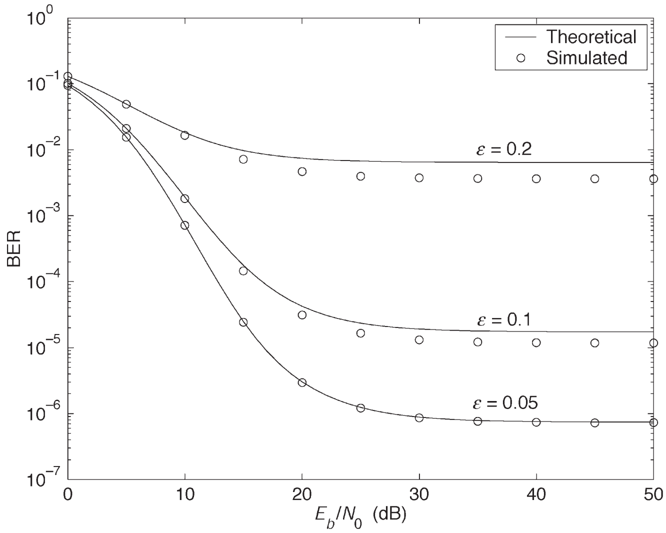

Fig. 5. BER of QPSK in the Rician channel D.

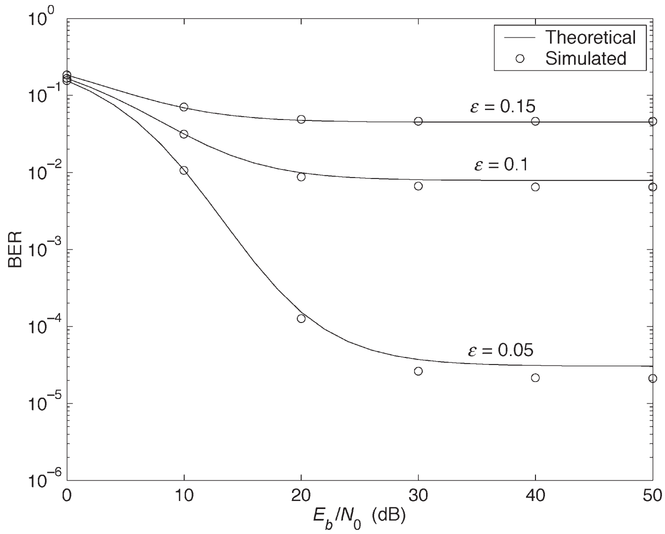

Fig. 6. BER of 16-QAM in the Rician channel D.

As a worst case for checking the Gaussian approximation, we considered the BER of the best subcarrier, because in this case, the number of subcarriers that contribute to the ICI is the smallest one. Anyway, Fig. 4 clearly evidences that the approximation is very accurate in this context too.

Figs. 5 and 6 illustrate the BER performance in the channel D with Rician factor $K = 10$, for QPSK and 16-QAM, respectively. In such a scenario, for high values of E_{b}/N_0, the theoretical BER, which is obtained by Monte Carlo integration of (47), is less accurate than in the previous cases. The reason for this inaccuracy is the high Rician factor K, which produces a high value of the channel mean value λ_{LOS}. Consequently, the term χ_1 in (43) is the dominant one among the ICI terms. Since χ_1 is similar to the ICI term in AWGN channels, we expect that the theoretical BER overestimates the true BER, as in AWGN channels [7]. Nevertheless, as shown in Figs. 5 and 6, in Rician channels, this mismatch is very small.

Fig. 7 shows the BER performance in the presence of a nonlinear HPA at the transmitter, when the normalized CFO is equal to $\varepsilon = 0.01$, using 16-QAM and the channel B. In the presence of nonlinear distortion, we define $E_{\mathrm{b}}/N_0 = c_{\lambda_1\lambda_1}(|A_0|^2 + \sigma^2_{\mathrm{NL}})/(\sigma^2_{\mathrm{AWGN}} \log_2 M)$, and the output backoff (OBO) as $B_{\mathrm{OUT}} = P_{\mathrm{U,MAX}}/\sigma^2_{\mathrm{U}}$, where $P_{\mathrm{U,MAX}}$ and σ^2_{U} are the maximum power and the mean power, respectively, of the HPA output signal. We assume that the amplifier is perfectly predistorted, i.e., it behaves as a clipper of the HPA input envelope. In this case, it holds true that $B_{\mathrm{OUT}} = B_{\mathrm{IN}}/(1 - \mathrm{e}^{-B_{\mathrm{IN}}})$ and that $A_0 = 1 - \mathrm{e}^{-B_{\mathrm{IN}}} + (\sqrt{\pi B_{\mathrm{IN}}}/2)\mathrm{erfc}(\sqrt{B_{\mathrm{IN}}})$ [23]. The results of Fig. 7 clearly indicate that the theoretical analysis is quite accurate also when both CFO and nonlinear distortions are present. Indeed, the Gaussian approximation of the nonlinear-distortion noise is quite accurate for low OBO, i.e., when the nonlinear-distortion noise dominates the ICI. On the contrary, if the OBO is high, the Gaussian approximation of the nonlinear-distortion noise is not very accurate for $N = 64$ active subcarriers [27]. However, at high OBO, the nonlinear-distortion noise is dominated by the ICI, whose pdf is well approximated by a Gaussian function.

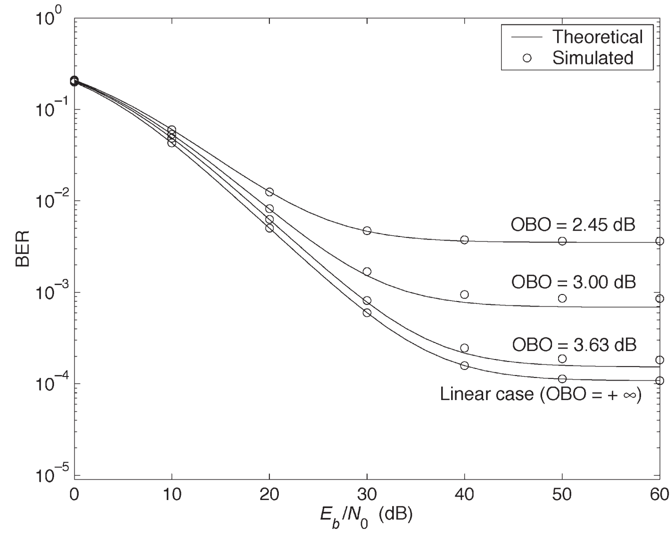

Fig. 7. BER of 16-QAM in the Rayleigh channel B when $\varepsilon = 0.01$.

Finally, we want to point out that the Gaussian approximation of the ICI can be successfully applied not only in WLAN scenarios, but also in broadcasting environments. Indeed, the OFDM systems usually employed for broadcasting applications have thousands of active subcarriers [1], and therefore, it is expected that the Gaussian approximation of the ICI will perform even better than in WLAN situations. Moreover, with thousands of active subcarriers, also the Gaussian approximation of the nonlinear-distortion noise is very accurate [23], [27], and therefore, the proposed approach is even more reliable.

VI. Conclusion

We have proposed a theoretical approach that allows the prediction of the BER of uncoded OFDM systems impaired by CFO in frequency-selective Rayleigh (or Rician) fading channels. We also considered the joint effect of CFO and nonlinear distortions introduced by a nonlinear amplifier at the transmitter. The proposed approach, based on the Gaussian approximation of the ICI, is not only characterized by a good degree of accuracy, but it has also the advantage of being very simple. Further studies could also consider the presence of channel estimation errors [10] and channel coding performed by linear precoders [28].

REFERENCES

[1] R. van Nee and R. Prasad, *OFDM for Wireless Multimedia Communications*. Boston, MA: Artech House, 2000.

[2] T. Pollet, M. van Bladel, and M. Moeneclaey, "BER sensitivity of OFDM systems to carrier frequency offset and Wiener phase noise," *IEEE Trans. Commun.*, vol. 43, no. 234, pp. 191–193, Feb./Mar./Apr. 1995.

[3] P. H. Moose, "A technique for orthogonal frequency division multiplexing frequency offset correction," *IEEE Trans. Commun.*, vol. 42, no. 10, pp. 2908–2914, Oct. 1994.

[4] B. Stantchev and G. Fettweis, "Time-variant distortions in OFDM," *IEEE Commun. Lett.*, vol. 4, no. 10, pp. 312–314, Sep. 2000.

[5] G. L. Stüber and M. Russell, "Terrestrial digital video broadcasting for mobile reception using OFDM," in *IEEE Global Telecommunications Conf.*, Singapore, Nov. 1995, vol. 3, pp. 2049–2053.

[6] J. Li and M. Kavehrad, "Effects of time selective multipath fading on OFDM systems for broadband mobile applications," *IEEE Commun. Lett.*, vol. 3, no. 12, pp. 332–334, Dec. 1999.

[7] T. Keller and L. Hanzo, "Adaptive multicarrier modulation: A convenient framework for time–frequency processing in wireless communications," *Proc. IEEE*, vol. 88, no. 5, pp. 611–640, May 2000.

[8] Y. Zhao and S. G. Häggman, "BER analysis of OFDM communication systems with intercarrier interference," in *IEEE Int. Conf. Communication Technology*, Beijing, China, Oct. 1998, vol. 2, pp. 1–5. S38-02.

[9] K. Sathananthan and C. Tellambura, "Probability of error calculation of OFDM systems with frequency offset," *IEEE Trans. Commun.*, vol. 49, no. 11, pp. 1884–1888, Nov. 2001.

[10] H. Cheon and D. Hong, "Effect of channel estimation error in OFDM-based WLAN," *IEEE Commun. Lett.*, vol. 6, no. 5, pp. 190–192, May 2002.

[11] M. Russell and G. L. Stüber, "Interchannel interference analysis for OFDM in a mobile environment," in *IEEE Vehicular Technology Conf.*, Chicago, IL, Jul. 1995, vol. 2, pp. 820–824.

[12] Z. Wang and G. B. Giannakis, "Wireless multicarrier communications: Where Fourier meets Shannon," *IEEE Signal Process. Mag.*, vol. 17, no. 3, pp. 29–48, May 2000.

[13] X. Ma, C. Tepedelenlioğlu, G. B. Giannakis, and S. Barbarossa, "Non-data-aided carrier offset estimators for OFDM with null subcarriers: Identifiability, algorithms, and performance," *IEEE J. Sel. Areas Commun.*, vol. 19, no. 12, pp. 2504–2515, Dec. 2001.

[14] T. M. Schmidl and D. C. Cox, "Robust frequency and timing synchronization for OFDM," *IEEE Trans. Commun.*, vol. 45, no. 12, pp. 1613–1621, Dec. 1997.

[15] H. Minn, M. Zeng, and V. K. Bhargava, "On timing offset estimation for OFDM systems," *IEEE Commun. Lett.*, vol. 4, no. 7, pp. 242–244, Jul. 2000.

[16] D. Landström, S. K. Wilson, J.-J. van de Beek, P. Ödling, and P. O. Börjesson, "Symbol time offset estimation in coherent OFDM systems," *IEEE Trans. Commun.*, vol. 50, no. 4, pp. 545–549, Apr. 2002.

[17] S. M. Kay, *Fundamentals of Statistical Signal Processing: Estimation Theory*. Englewood Cliffs, NJ: Prentice-Hall, 1993.

[18] A. Papoulis, *Probability, Random Variables and Stochastic Processes*, 3rd ed. New York: McGraw-Hill, 1991.

[19] K. Cho and D. Yoon, "On the general BER expression of one- and two-dimensional amplitude modulations," *IEEE Trans. Commun.*, vol. 50, no. 7, pp. 1074–1080, Jul. 2002.

[20] M. Abramowitz and I. A. Stegun, *Handbook of Mathematical Functions*, 9th ed. New York: Dover, 1970.

[21] L. Rugini and P. Banelli. (2003, Dec.). "Symbol error probability of linearly modulated signals affected by Gaussian interference in Rayleigh fading channels," *RT-005-03*, Dept. Electron. Inform. Eng., Perugia, Italy, pp. 1–18. [Online]. Available: http://www.diei.unipg.it/rt/DIEI_RT.htm

[22] I. S. Gradshteyn and I. M. Ryzhik, *Table of Integrals, Series, and Products*, 5th ed. San Diego, CA: Academic, 1994.

[23] P. Banelli and S. Cacopardi, "Theoretical analysis and performance of OFDM signals in nonlinear AWGN channels," *IEEE Trans. Commun.*, vol. 48, no. 3, pp. 430–441, Mar. 2000.

[24] D. Dardari, V. Tralli, and A. Vaccari, "A theoretical characterization of nonlinear distortion effects in OFDM systems," *IEEE Trans. Commun.*, vol. 48, no. 10, pp. 1755–1764, Oct. 2000.

[25] A. Doufexi, S. Armour, M. Butler, A. Nix, D. Bull, J. McGeehan, and P. Karlsson, "A comparison of the HIPERLAN/2 and IEEE 802.11a wireless LAN standards," *IEEE Commun. Mag.*, vol. 40, no. 5, pp. 172–180, May 2002.

[26] Z. Wang and G. B. Giannakis, "What determines average and outage performance in fading channels?," in *IEEE Global Telecommunications Conf.*, Taipei, Taiwan, R.O.C., Nov. 2002, vol. 2, pp. 1192–1196.

[27] H. Nikopour and S. H. Jamali, "Effects of Cartesian clipping noise on the performance of orthogonal frequency division multiplexing system: A theoretical approach," in *IEEE Global Telecommunications Conf.*, Taipei, Taiwan, R.O.C., Nov. 2002, vol. 2, pp. 1254–1258.

[28] Z. Liu, Y. Xin, and G. B. Giannakis, "Linear constellation precoding for OFDM with maximum multipath diversity and coding gains," *IEEE Trans. Commun.*, vol. 51, no. 3, pp. 416–427, Mar. 2003.

Luca Rugini (S'01–M'05) was born in Perugia, Italy, in 1975. He received the Laurea degree in electronics engineering and the Ph.D. degree in telecommunications from the University of Perugia, Perugia, Italy, in 2000 and 2003, respectively.

He currently is a Postdoctoral Researcher with the Department of Electronic and Information Engineering, University of Perugia. His research interests include spread spectrum and multicarrier communications.

Paolo Banelli (S'90–M'99) was born in Perugia, Italy, on May 19, 1968. He received the Laurea degree in electronics engineering and the Ph.D. degree in telecommunications from the University of Perugia, Perugia, Italy, in 1993 and 1998, respectively.

He has been an Assistant Professor with the Department of Electronic and Information Engineering (DIEI), University of Perugia, since 1998. He visited the Department of Electrical and Computer Engineering (ECE), University of Minnesota, Minneapolis, from March to September 2001. His research interests include nonlinear distortions, broadcasting, and block transmission techniques for wireless communications.